Impact of Linear Array Geometry on Direction-of-Arrival Estimation for a Single Source

Edward J. Vertatschitsch, *Member, IEEE*, and Simon Haykin, *Fellow, IEEE*

Abstract—**The impact of the linear array geometry on the direction of arrival estimation accuracy is examined assuming a single source of illumination and additive white Gaussian system noise. The analysis was conducted using the Cramer–Rao lower bound (CRLB), simulations and performance modeling of maximum likelihood estimation (MLE). Particular attention is paid to the implementation of the MLE, the threshold signal-to-noise ratio (SNR), probability of outlier and high SNR mean-squared error (MSE) performance which are evaluated and compared for uniform and nonuniform arrays. The conditions under which trade-offs exist in choosing a particular geometry and their significance are determined.**

I. Introduction

A linear array structure consists of a finite number of sensors arranged in a single dimension. At a given instant in time, a narrow-band plane wave originating from a target in the far field of the array may be represented by the mathematical model of the complex envelope at the ith sensor as

$$s_i = a \exp\{j(\theta + 2\pi \sin(\phi) x_i/\lambda)\} \tag{1}$$

where

λ = radio wavelength,
ϕ = elevation angle,
a = amplitude of the signal,
θ = unknown phase shift,

and x_i is the location of the ith sensor in space. The quantity $2\pi \sin(\phi)/\lambda$ is referred to as the projected wavenumber, or just simply, wavenumber, henceforth it will be represented by the symbol k. The expression for the signal at the ith sensor may then be simplified as

$$s_i = a \exp\{j(\theta + kx_i)\}. \tag{2}$$

Since the wavelength λ acts merely as a scale factor in the estimation problem, we may develop a normalized system of parameters that is independent of λ. We then measure the sensor locations in units of $\lambda/2$. This implies that the smallest spacing in the array must be less than or equal to one unit in the normalized system. In turn, the normalized wavenumber is restricted to lie in the range $(-\pi, \pi)$. The normalized wavenumber has an alternative interpretation. The value k is now exactly equal to the observed phase difference (in radians) between two elements that are separated by the minimum spacing of one unit.

In an electronically agile array requiring maximum sensitivity, each sensor requires a separate receiver. For large numbers of elements, the overall cost of the array is dominated by the cost of the active elements and may become prohibitively expensive. Since the field of view constrains the minimum spatial sampling rate, it may be possible to decrease the beamwidth to less than that of a uniform array using nonuniform spacing. It then becomes a question of maximizing performance for a given, finite number of sensors (cost) by varying the array geometry.

In this paper, we are primarily concerned with high-accuracy estimation in the context of a single source of illumination with a single temporal snapshot. (A companion paper [1] discusses the effect of multipath.) In particular we are interested in wavenumber estimation accuracies significantly better than a beamwidth. This objective is attained by a judicious placement of the sensors. The array geometry's impact on estimator performance and the trade-offs encountered in choosing certain configurations would therefore need to be investigated.

The paper is organized as follows. Section II provides a brief background of the development of nonuniform arrays. Section III describes the maximum likelihood estimator (MLE) and Section IV describes the implementation requirements for optimal performance. In Section V, we examine the single-target location problem using simulations with the MLE for uniform and nonuniform arrays. In Section VI, we compare the figures of merit and summarize the impact of array geometry on the direction finding problem. The results build upon concepts first described in the classic paper by Rife and Boorstyn (R–B) [2]. Their basic discussion of the estimation error dealt exclusively with uniform structures. Those concepts are extended here to arbitrary array configurations, of which the uniform array is a special case.

II. Background

The literature provides a rich assortment of descriptions for the structures in which the spacing between elements is unequal. Some of the most common are: nonuniform, sparse,

Manuscript received October 14, 1988; revised September 20, 1990.
E. J. Vertatschitsch was with the Communications Research Laboratory, McMaster University, Hamilton, ON, Canada. He is now with the Boeing Company, P.O. Box 3999, Seattle, WA 98124.
S. Haykin is with the Communications Research Laboratory, McMaster University, Hamilton, ON, L8S 4K1 Canada.
IEEE Log Number 9143712.

0018-926X/91/0500-0576$01.00

TABLE I
ARRAYS TO BE EVALUATED

Number of Sensors	Location										Array Property
5	0	1	2	3	4						U
	0	1	4	7	9						MR
	0	2	7	8	11						NR & UR
6	0	1	2	3	4	5					U
	0	1	2	6	10	13					MR
	0	1	4	10	12	17					NR & UR
7	0	1	2	3	4	5	6				U
	0	1	2	6	10	14	17				MR
	0	6	9	10	17	22	24				UR
	0	1	4	10	18	23	25				NR
8	0	1	2	3	4	5	6	7			U
	0	1	2	11	15	18	21	23			MR
	0	8	18	19	22	24	31	39			UR
	0	1	4	9	15	22	32	34			NR
9	0	1	2	3	4	5	6	7	8		U
	0	1	2	14	18	21	24	27	29		MR & UR
	0	1	5	12	25	27	35	41	44		NR
10	0	1	2	3	4	5	6	7	8	9	U
	0	1	3	6	13	20	27	31	35	36	MR
	0	7	22	27	28	31	39	41	57	64	UR
	0	1	6	10	23	26	34	41	53	55	NR

U—uniform, MR—minimum redundant, UR—unrestricted, NR—nonredundant

thinned, aperiodic, and space-tapered arrays. In addition, many authors simply refer to the structures according to the class construction or array design algorithm. In the 1960's, the advantages of eliminating the restriction of equal spacings became apparent. One of the prime motivations was the reduction of the number of elements required to obtain a desired antenna beam pattern, primarily for sidelobe reduction, referred to as thinning. Another common application of nonuniform arrays was the increase in the effective bandwidth through variable spacing, called broad-banding the array. The "optimum" array structure is very specific to the particular problem being considered. The formulation of the constraints greatly influences the final solution. In very few formulations was a closed-form solution found. A good summary of the early work on nonuniform arrays is provided in [3].

One of the first studies of redundancy construction of nonuniform arrays is that of Moffet [4], in which the case is made for maximizing the resolution of an array for a given number of sensors. The structures discussed, are actually those proposed by Leech [5], in a mathematical paper whose original intent was not the array problem. In these constructions we do not impose an aperture-length constraint on the array. Rather, for a given number of sensors, one or more "best" arrays are proposed. The conceptual solution is straightforward; however, the procedure is difficult and computationally intensive to implement for large numbers of elements. Therefore, suboptimal ways of extending these structures for very large numbers of elements have also been proposed [6]. Recently, the minimum-redundant arrays cited by Moffet have been obtained from other interpretations as well [7], [8].

An alternative procedure to the minimum redundant sampling was proposed in [9] and is known as a nonredundant construction. The grid-search method provided a set of arrays that were very nearly the minimum-length arrays having zero redundancy. Other algorithms have been developed which generate the minimum redundant arrays exhaustively and with minimal computational effort [10]–[14].

Unfortunately, the literature lacks a detailed study comparing performance of the redundancy-based array structures. Moreover, no consideration has been given to the trade-offs involved in choosing one of these thinned arrays over a uniform array. It is this impact of array geometry which we wish to explore in this paper and, thereby, provide a comprehensive understanding of the behavior of nonuniform arrays for the direction-of-arrival estimation problem. Table I provides a description of the nonuniform arrays that will be evaluated in the remainder of the paper.

III. Maximum Likelihood Estimation

We follow a similar approach to that provided by R–B [2], where the concepts were developed for the frequency estimation problem using uniformly sampled time-domain data. Many of their ideas are generalized here for arbitrary linear array structures. Briefly, the problem is the determination of an estimate of the wavenumber from noisy data. We assume that the target wavenumber and complex amplitude are unknown parameters represented by k_t and c_t, respectively. The normalized wavenumber is assumed to lie in an interval $(-\pi, \pi)$. The signal received at the ith sensor is given by

$$z_i = a \exp\{j(\theta + k_t x_i)\} + w_i \tag{3}$$

where w_i is complex additive white Gaussian noise, with statistically independent real and imaginary components. The MLE of wavenumber for a single target namely, $\hat{k}$, reduces

to that of obtaining the value of k that maximizes the objective function

$$\Lambda(k) = \left| \sum_{i=1}^{N} z_i \exp\{-jkx_i\} \right|^2. \quad (4)$$

When the x_i are uniformly spaced, (4) is recognized as the discrete Fourier transform (DFT) of the received data $\{z_i\}$. For nonuniform arrays in which the sensors lie on an integer grid, the expression may be interpreted as a padded DFT. Specifically, the received data vector may be padded with zeros wherever a sensor location is missing.

Several techniques exist for bounding the mean-squared error (MSE) of this problem. We will concentrate on the Cramer–Rao lower bound (CRLB) for unbiased estimators [15], which has been shown to be valid for sufficiently large signal-to-noise ratio (SNR). Let Γ be defined as the elemental SNR:

$$\Gamma = |c_t|^2/(2\sigma^2) \quad (5)$$

where $2\sigma^2$ is the white noise power. Application of the CRLB results in bounding the variance of any unbiased estimator as

$$\text{var}\{(k_t - \hat{k})\} \geq (2\Gamma S)^{-1} \quad (6)$$

where the spread is given by $S = \Sigma(x_i - C)^2$ and C is the centroid of the array given by $\Sigma x_i/N$. The threshold SNR is defined as the value of SNR for which the MSE of the estimator differs from the CRLB by 1 dB.

The maximization of (4) is a nonlinear problem. We initially search the wavenumber space on a coarse grid, determining the approximate location of the maximum. Upon locating this point, a fine grid search is then performed over the coarse intervals on either side. The fine search is repeated in multiple levels until the desired accuracy in estimation is obtained.

The objective of the coarse search is to locate the global maximum. In this way, the fine searches are implemented assuming the surface to be convex over the previous search interval. This then necessitates some knowledge of the density required for the coarse search. The determination of a sufficient density is made from a statistical viewpoint. A given performance measure is evaluated using a large number of simulations for each of several coarse search densities. At the point for which the measure does not change significantly, we say that for practical purposes, the coarse search density is adequate.

In their work, R–B [2] concluded a density of N points in 2π was adequate for uniform arrays of N elements in which the MSE as a function of SNR was used as the performance measure. In this paper, we show that this particular choice of experimental framework predicted a density and performance that is overly optimistic in its determination of the threshold SNR and the probability of outlier. The derivations and simulations that supported these findings were performed for a fixed frequency, and the coarse search estimates were made at uniform spacings, one of which coincides with the true location of the tone. When only N coarse search points in 2π were used, the remaining points fell at the nulls (in the absence of noise) of the DFT. This is obviously a fortuitous circumstance that cannot be expected to occur in our problem. In general, none of the coarse search points will coincide with the true location of the tone frequency, and many may also be located near the peaks of sidelobes of the DFT. In the next section we extend the R–B concepts to nonuniform arrays.

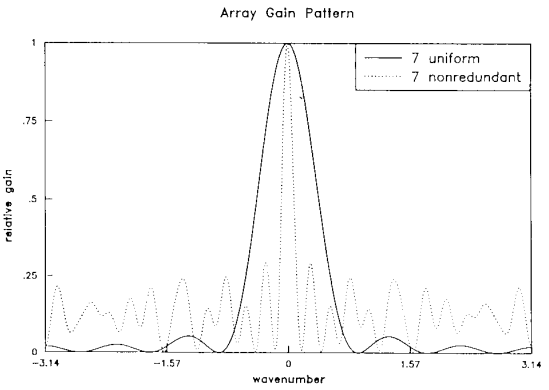

Fig. 1. Comparison of the standard gain patterns associated with seven-element uniform and nonredundant arrays.

It is of interest to examine the beam pattern of the array structure. The beam pattern, or array power gain pattern in our notation, is defined by

$$G(k) = \left| \frac{1}{N} \sum_{i=1}^{N} \exp\{jkx_i\} \right|^2 \quad (7)$$

with k varying over the interval $(-\pi, \pi)$. This result is proportional to that obtained for the objective function of the MLE operating in infinite SNR when the target is at boresight, $k_T = 0$, as given in (4). The beam patterns for seven-element uniform and nonredundant arrays, described in Table I, are presented in Fig. 1. The pattern for the uniform array is very regular, with sidelobes tapering as the distance from boresight increases. The nonredundant array's behavior, on the other hand, is somewhat more erratic, with the peak sidelobe being relatively larger than its uniform counterpart. The other principal observation discerned from Fig. 1 is a significant reduction in the width of the main lobe for the nonredundant array. The standard beamwidth, in physical space (measured in radians), for an aperture of size L is defined as λ/L. Translated to the normalized wavenumber space, it becomes $2\pi/A$ where A is the ratio of L to the minimum spacing used.

IV. MLE Implementation Requirements

From (4) and Fig. 1, we see that the objective function will have multiple maxima. The coarse search must be dense enough such that the maximum located should correspond to a point on the main lobe. Under "noisy" conditions, it is difficult to determine the required density that would guarantee this; however, we may use a pragmatic approach. The density will be assumed adequate if the "average" perfor-

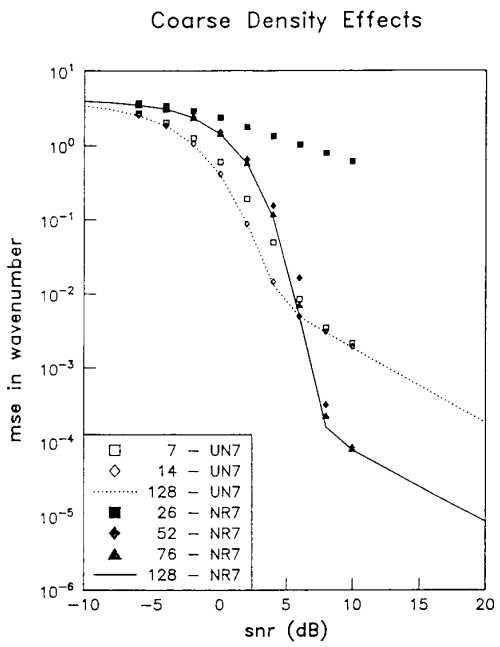

Fig. 2. Effects of the coarse search density on the performance estimation of seven-element uniform and nonredundant arrays.

mance (i.e., mean-square estimation error, or threshold SNR), is not degraded. The result of [2] for uniform arrays, in which a density of N coarse points for the N element uniform array was used, is effectively one sample per beamwidth. As an initial starting point, we could consider a similar density for the coarse search. We expect that since the nonredundant arrays have larger sidelobe levels, they will require higher densities than the corresponding uniform arrays.

The MSE for the two seven-element arrays is presented in Fig. 2 for different coarse search densities. The target wavenumber was varied over an interval of $(-\pi/2, \pi/2)$, and the search was carried out over $(-\pi, \pi)$, using $2^{16} = 65536$ simulations for each value of SNR and coarse search density. This variation in wavenumber was used to prevent the true wavenumber always coinciding with one of the coarse sampling points. After locating the coarse maximum position, a fine-grid search was performed extending one interval to either side of the candidate position. The simulations were carried out primarily in the threshold regions in order to clearly observe the effect.

The results with the seven-element uniform array show a density of 14 points to provide sufficient accuracy in determining the variation of MSE as a function of SNR. For large SNR, seven points distributed over 2π were found to be sufficient to reach the CRLB. In the threshold region, the seven-point coarse search requires up to an additional 1 dB in SNR. This demonstrates the necessity of using more points in the coarse search for an accurate characterization of performance when the target position may lie at any point within an interval. The fact that in [2] all but one of the sampling points occurred at the nulls of the beam pattern permitted a simple,

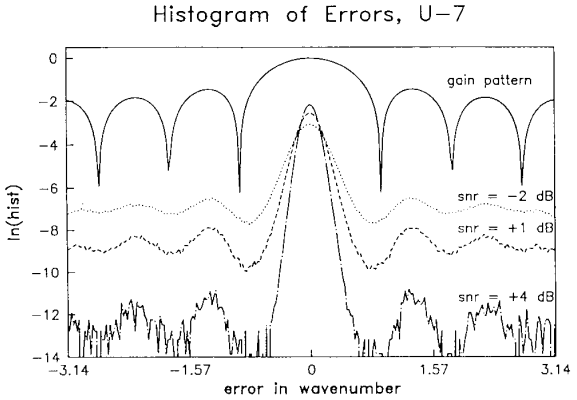

Fig. 3. Histogram of estimation errors for three different values of SNR using a seven-element uniform array. Superimposed is the standard beam pattern.

analytical derivation of outlier performance. This will be reexamined later in the paper.

Turning next to the nonredundant array, the results indicate that for a coarse search having two points per beamwidth the threshold region is increased by approximately 0.5 dB in SNR. For a density of three points per beamwidth, the performance is in agreement with the higher densities within statistical accuracies. This increased density requirement was expected as the peak sidelobe levels of the estimator power gain pattern are larger than in the uniform array and it is therefore more difficult to ascertain the particular lobe having the global maximum.

It is important to note that for both the uniform and nonuniform arrays, when the high density coarse search was implemented the estimator performance was virtually unaffected (within statistical uncertainty) by varying the target location. Therefore, the results would have been similar if the target were restricted to boresight only. The effect was only clearly visible when one sample per beamwidth was used in the coarse search, in which case the exact locations of the target signal and the coarse search test points were critical.

The examination of the maximum likelihood estimator in the threshold region provides meaningful insight into the error process. The probability density function of the wavenumber estimation error is gauged from simulation results by generating a histogram of the errors. For each value of SNR, $2^{20} = 1\,048\,576$ estimates of the wavenumber were generated. During each investigation, two histograms were accumulated. The first involved 256 bins covering the region of $(-\pi, \pi)$. The second consisted of 64 bins spread over the "main beam" covering the interval $(-B/2, B/2)$ where B is the beamwidth defined earlier as $2\pi/A$.

The results shown in Figs. 3 and 4 compare the arrays U7 and NR7. The experiments were performed at the same elemental SNR values, -2, $+1$, and $+4$ dB. For clarity, the $+1$ dB SNR was not displayed for the nonredundant array in Fig. 4. The histogram was normalized by dividing the count in each bin by the total number of trials. The logarithm of the antenna gain pattern is presented as the solid curve in each figure for comparison.

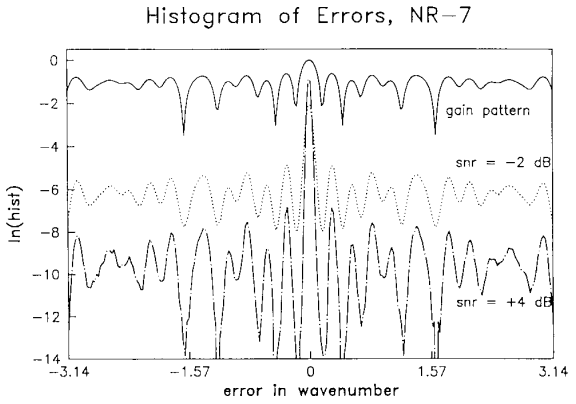

Fig. 4. Histogram of estimation errors for two different values of SNR using a seven-element nonredundant array. Superimposed is the standard beam pattern.

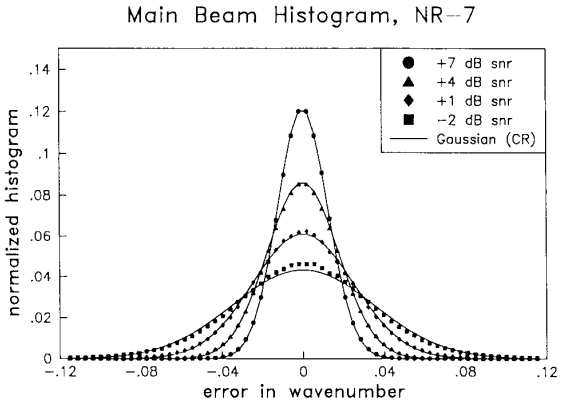

Fig. 6. Expanded histogram of the region associated with the main lobe of the gain pattern for a seven-element uniform array. Included is the equivalent Gaussian probability distribution.

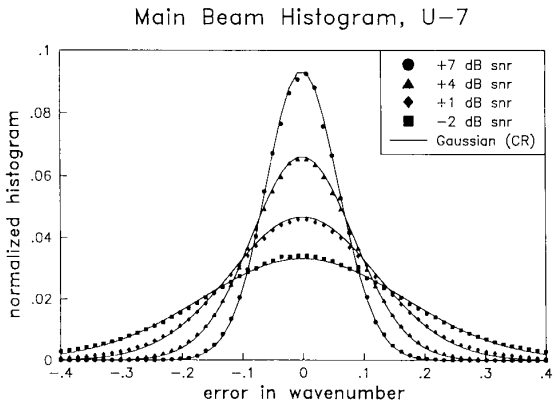

Fig. 5. Expanded histogram of the region associated with the main lobe of the gain pattern for a seven-element uniform array. Included is the equivalent Gaussian probability distribution.

The estimator, defined in (4), is closely related to the gain pattern, defined in (7). Both Figs. 3 and 4 indicate that large errors are more likely to occur near a peak of the sidelobe gain pattern than at the null. In other words, noise increases the likelihood of one of the sidelobes being greater than the area surrounding the main beam. When this occurs, the error is termed an outlier. The probability of an outlier is defined as the probability that the error in wavenumber falls outside the main beam of the array.

For errors within the beamwidth of the array, the performance is more conventional as shown in Figs. 5 and 6. Specifically, we may state the following: 1) for large SNR's, the predicted performance may be modeled as a Gaussian distribution of zero mean and variance given by the Cramer-Rao lower bound; 2) for low SNR values, the Gaussian distribution is not as good an approximation since the CRLB standard deviation becomes comparable to the beamwidth of the array.

While the mean square error is certainly an important measure of performance, it is not the only consideration. We can also view the errors as coming from one of two distributions. With probability p_0 (a function of SNR), it is an outlier, and with probability $(1 - p_0)$ it is Gaussian distributed with variance given by the CRLB. The threshold SNR is determined to be the minimum SNR at which the system should be operated. Rather than choose the point for which the MSE is 1 dB greater than the CRLB, an array designer may require a certain maximum probability of outlier occurrence. When an outlier occurs, it is almost as likely to make extremely large errors as it is to make them just outside a beamwidth. In this region, the probability does not fall off as a Gaussian would, and the existence of very large errors may be critical to the designer.

We return to the model used by R-B [2], for which an N-point coarse search was implemented on an N-element uniform array. Provided one of the coarse search points falls on the true target location, their definition of outlier is the event for which one of the incorrect values of the coarse search would provide a greater value of the objective function than the one corresponding to the true location. These assumptions allow the probability of outlier to be calculated analytically and the result [2, eq. 60] is reproduced here (using our notation) as

$$p_0 = \frac{1}{N} \sum_{m=1}^{N} \frac{N!\,(-1)^m}{(N-m)!\,m!} \exp\left\{-N\Gamma \frac{(m-1)}{m}\right\}. \quad (8)$$

For high SNR, the equation is dominated by the term $m = 2$

$$p_0 \simeq \frac{N-1}{2} \exp\{-N\Gamma/2\} \quad (9)$$

or taking logarithms,

$$\ln(p_0) \simeq -\frac{N}{2}\Gamma + \ln((N-1)/2). \quad (10)$$

This approximation is asymptotically tight with increasing SNR. The probability of outlier given by (8) and the approximation given by (9) are in reasonable agreement for values of p_0 as large as 0.01 for arrays of the size considered here.

Unfortunately this definition of an outlier is specific to a particular set of parameter circumstances. In general, the

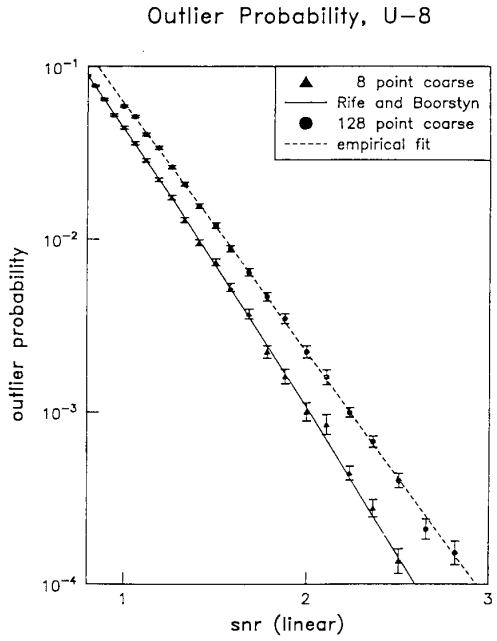

Fig. 7. Probability of outlier for an eight-element uniform array showing the overly optimistic results obtained using [2]; "true" performance is indicated by the 128 point coarse search.

target will not coincide with one of N points in the coarse search region, and therefore we find an increased number of points are required in the initial grid search. Finally, it is also not suitable for extensions to nonuniform arrays.

We will show, however, that the trend indicated by (9) is nevertheless accurate for the general problem of arbitrary location of the target for uniform and nonuniform arrays. That is, for $p_0 < 0.01$, we find that the probability of outlier decreases as a simple exponential in SNR.

V. Results

We begin by considering the result for uniform arrays. Positioning the target at boresight, and using a proper search implementation, we determine the probability of outlier versus SNR. As a point of reference, and to validate the previous expressions, we also implement the search described in [2]. The results are presented in Fig. 7 for the eight-element uniform array, for which we plot p_0 (on a logarithmic scale) versus Γ (on a linear scale). The error bars shown in Fig. 7 are the estimates of the standard deviation of the value of $\log(p_0)$, determined statistically.

The solid curve in Fig. 7 is a plot of (10) which fits the eight-point coarse search quite well. The "true" performance is indicated through the use of a 128-point coarse search. For $p_0 < 0.01$, we fit $\ln(p_0)$ to a linear curve in SNR. The results of the calculation are displayed as the empirical fit in Fig. 7. The fitting was performed as a weighted least-squares fit using orthogonal polynomials.

The probabilities of outlier were found in two stages, initially using 2^{14}-point simulations which would provide reasonably accurate estimates of the probabilities in the larger regions of p_0. The region having lower values of p_0 were then simulated again with a greater number of trials. The fitting process used those data points for which $p_0 < 0.01$, and at least 25 outliers occurred. The 25-outlier requirement restricts the range of p_0 to values above $25/N_S$, where N_S is the number of simulations. Typically, for N_S equal to 2^{18}, this translates to fitting values of p_0 in the region $10^{-4} < p_0 < 10^{-2}$. The error bars plotted are estimates of the root mean square (RMS) uncertainty of the observed quantity.

We observe from Fig. 7: 1) although the values of $p_0 > 0.01$ were not chosen for the fitting, they still lie very close to the empirical curve for values of p_0 as large as 0.1; and 2) the R-B simulations were optimistic, both in the probability of outlier and the rate at which it falls off. Their result predicted a curve in this region of SNR to be of the shape

$$p_{RB} \simeq 3.5 \exp(-4\Gamma) \simeq \exp(1.25 - 4\Gamma). \quad (11)$$

The fit (we performed) indicates the true behavior to be

$$p_0 \simeq \exp(a + b(\Gamma - \beta)) \simeq \exp(0.53 - 3.318\Gamma) \quad (12)$$

where

$$a = -5.830 \pm 0.020 \quad (13)$$

$$b = -3.318 \pm 0.062 \quad (14)$$

and

$$\beta = 1.9150. \quad (15)$$

The value of β was chosen such that the quoted standard deviations of uncertainty in a and b are uncorrelated. The intercept

$$a - b\beta = 0.53 \pm 0.12 \quad (16)$$

and the slope coefficient b from (14), are shown to be significantly poorer under the general conditions of the source location problem than is obtained by using the R-B results directly.

A similar analysis of simulation results for the seven-element nonredundant array is now made. The observed probability of outlier and the exponential fits are presented in Fig. 8, which clearly shows the increased probability of outlier for the nonredundant array. Not only is it larger, but it also falls off at a slower rate with SNR than it does for the uniform array. We may define a new threshold SNR for architecture comparisons as the point at which the probability of outlier equals a required specification. This provides a critical measure in evaluating array structures for specific applications.

Using the fit results, we can invert the function to find the expected SNR corresponding to the required p_0. For values of p_0 within the fitting range, this will be an interpolation with very accurate results. However, we may now also extrapolate to much lower values of p_0 than could be easily observed. For these results, the estimated error of extrapolation grows as the value of p_0 decreases. The advantages of this technique for moderate extrapolations will be a reasonable estimate of threshold SNR, for which the outlier probability may be impractical to simulate. It also provides an estimate of the required SNR, and once a designer has narrowed down the array configurations to be considered, a more accurate simulation may be performed.

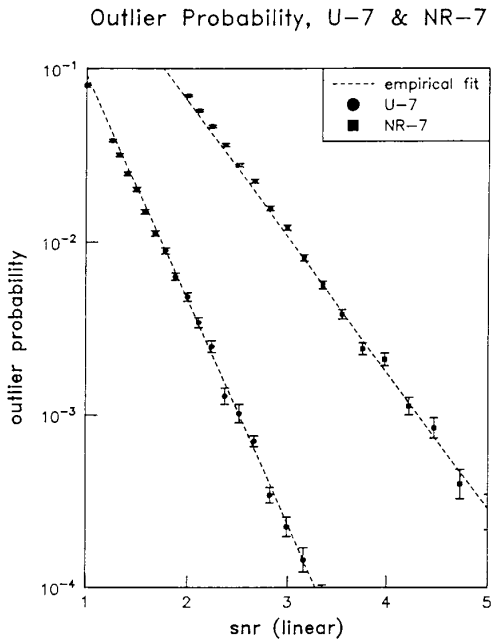

Fig. 8. Empirical fitting of the outlier probability determined by simulation for seven-element uniform and nonredundant arrays.

The selected arrays described in Table I, are examined for the probability of outlier variation with SNR. The statistical error analysis and goodness of fit criteria are discussed in [16] where the model is found to be justified within the statistical errors based on a large number of these experiments. There did not appear to be any correlation with the number of elements or with the array structure. From these results, we feel justified in proposing the single exponential fit for probability of outlier versus SNR for sufficiently low values of p_0.

The observations are reproduced in Table II. For each array, the interpolated/extrapolated array SNR corresponding to values of p_0 equal to 10^{-3} and 10^{-6} are determined from the inverse of the fit. For all arrays, the accuracy of the inverse fit at $p_0 = 10^{-6}$ is better than 0.1 dB in SNR, while at 10^{-3} it was accurate to better than 0.05 dB.

In Table II, we have introduced the new term, sampling gain. It is defined as the savings in SNR (in decibels) required to obtain a given single-target MSE performance for the array under consideration when compared to a uniformly sampled array consisting of an equal number of elements and an equivalent field of view. The sampling gain is independent of the value of the MSE chosen since the calculation is made at values of the SNR beyond the threshold region at which the CRLB may be used to determine performance. If the minimum spacing is chosen to be one unit for both the uniform and nonuniform arrays consisting of N elements, the sampling gain becomes

$$G_s = 10\log(S) - 10\log\left(N(N^2 - 1)/12\right) \quad (17)$$

where the spread of the array under consideration, S, was defined in (6). The significance of the sampling gain is that the expected savings in SNR (for a required MSE performance) may be translated into improved performance such as: greater range for a given output power; improved estimation accuracy for a given quality of receiver; or it may be used to reduce the number of elements and the cost of the array. We show a potential savings of 16.6 dB in elemental SNR is available when comparing 10-element uniform and nonredundant arrays. For a sufficiently large SNR such that both arrays were operating at their respective CRLB's, the accuracy improvement is approximately a factor of 45 for the same elemental SNR.

VI. Discussion

It is interesting to compare the arrays of different numbers of elements and which is the reason for using the array SNR, $N\Gamma$ and not the elemental SNR, Γ. We obtain the interesting result that, for all uniform arrays measured, for $p_0 = 10^{-6}$, the required array SNR is 15.4 dB ± 0.1 dB; this includes five- to 32-element uniform arrays. In this region, the required array SNR is virtually independent of the number of elements. We find it is also possible to make similar statements about the nonuniform arrays. All minimum redundant arrays, labeled MR, required 17.2 ± 0.1 dB of array SNR, again well within the measurement accuracy. The nonredundant arrays required 17.3 dB ± 0.3 dB in all cases. We note that these arrays extend from 11 to 55 units of length.

The behavior for the eight- and 10-element unrestricted arrays using the MLE is particularly interesting. They require larger apertures, provide less sampling gain and have poorer threshold SNR values than the equivalent nonredundant arrays. We may therefore conclude that there is no advantage in choosing these arrays over the nonredundant ones. That is, even though the required aperture is larger, the array geometry is inefficient in terms of mean squared error performance and threshold SNR.

The nonredundant arrays generally exhibit a threshold performance not larger than 0.3 dB in excess of the minimum redundant arrays and yet provide up to an additional 3 dB of MSE reduction (for $N = 10$). Generally, we would expect that the nonredundant arrays would be preferred over the other nonuniform arrays considered. In terms of probability of outlier, the results are similar. The significant trade-off is for the uniform arrays versus the nonredundant ones. The nonredundant arrays require approximately a 2 dB larger elemental SNR to provide the same probability of outlier as the uniform arrays. The benefit is an improved MSE at the higher SNR values ranging from 9.1 dB for the case $N = 5$, to 16.6 dB for $N = 10$. That is, provided the data can be averaged (filtered) for the additional time, or if the SNR is above the critical point for one snapshot, the 10-element nonredundant array will provide a mean square estimation error 45 times smaller than the 10-element uniform array.

As mentioned earlier, the increased probability of outlier for the nonuniform arrays is due to the increased sidelobe level. In situations in which multiple temporal snapshots may be used, it is possible to effectively reduce the sidelobe problem and hence the outlier probability using other techniques (Capon's method) as described in [17].

TABLE II
SAMPLING GAIN AND THRESHOLD COMPARISON USING ARRAY SNR, $N\Gamma$

Number of Sensors	Array[1] Type	Sampling Gain (dB)	$p = 10^{-3}$ @ SNR (dB)[2]	$p = 10^{-6}$ @ SNR (dB)[2]	Threshold[3] SNR (dB)
5	U	0.0	12.4	15.4	12.6
	MR	7.7	14.4	17.3	15.7
	NR & UR	9.1	14.5	17.3	16.0
6	U	0.0	12.4	15.5	12.7
	MR	9.0	14.4	17.1	15.9
	NR & UR	11.2	14.6	17.4	16.3
7	U	0.0	12.5	15.3	13.0
	MR	9.8	14.5	17.3	14.2
	UR	12.1	14.6	17.3	16.4
	NR	13.7	14.8	17.6	17.0
8	U	0.0	12.5	15.4	13.2
	MR	11.7	14.5	17.2	16.4
	UR	14.0	14.6	17.3	16.7
	NR	14.9	14.6	17.1	16.6
9	U	0.0	12.6	15.4	13.3
	MR & UR	11.7	14.5	17.2	16.5
	NR	15.9	14.5	17.1	16.7
10	U	0.0	12.6	15.5	13.5
	MR	13.5	14.4	17.1	16.6
	UR	16.3	14.5	17.0	16.8
	NR	16.6	14.5	17.0	16.7
16	U	0.0	12.8	15.4	14.0
32	U	0.0	13.0	15.4	14.6

[1] Arrays correspond to those listed in Table I.
[2] Array SNR, $N\Gamma$, required to obtain specified probability of outlier, determined from empirical fit.
[3] Threshold array SNR determined by MLE for target at boresight and search over $(-\pi, \pi)$.

VII. SUMMARY

The results of the research reported herein indicate that a trade-off in performance measures may be required when choosing a particular geometry. A significantly improved mean squared error performance may be achieved due to the larger aperture of nonuniform arrays, although the actual geometry is still important. However, this is accompanied by a modest increase in the threshold SNR for these arrays, primarily due to increased sidelobe levels. The probability of outlier also increases for the same reason.

The sampling gain, defined as the savings in SNR for achieving a specified MSE at high SNR could be obtained directly from the CRLB (MLE estimation coincided with the CRLB for sufficiently large SNR). In the event of single targets in additive white Gaussian noise, the sparse arrays provide significant improvement over uniform arrays of the same number of elements and the same field of view.

The trade-off occurs when additional performance estimators are considered such as the probability of outlier defined as the probability of an estimation error greater than the beamwidth of the array. The probability of outlier can be approximated by a simple negative exponential in SNR for values of $p_0 < 0.01$. For single target problems, the uniform arrays have lower values of p_0 in this region and decrease more rapidly with increasing SNR than for the sparse arrays. This outlier probability was shown to account for the threshold effect in MSE and therefore similar statements apply.

In general the nonredundant arrays provided improved MSE improvements with virtually identical outlier performance when compared to minimum redundant designs, and therefore will usually be the design of choice. For an outlier probabilities of one part in one million, the nonredundant arrays required 2 dB greater SNR than uniform arrays but could provide up to 16.6 dB improvement in MSE (for $N = 10$).

REFERENCES

[1] E. J. Vertatschitsch and S. Haykin, "Impact of linear array geometry on direction of arrival estimation in the presence of multipath," in preparation.
[2] R. C. Rife and R. R. Boorstyn, "Single-tone parameter estimation from discrete-time observations," *IEEE Trans. Inform. Theory*, vol. IT-20, pp. 591–598, Sept. 1974.
[3] Y. T. Lo and S. W. Lee, "A study of space-tapered arrays," *IEEE Trans. Antennas Propagat.*, vol. AP-14, pp. 22–30, Jan. 1966.
[4] A. T. Moffet, "Minimum-redundancy linear arrays," *IEEE Trans. Antennas Propagat.*, vol. AP-16, pp. 172–175, Mar. 1968.
[5] J. Leech, "On the representation of $1, 2, \cdots, n$ by differences," *J. Lond. Math. Soc.*, vol. 31, pp. 160–169, 1956.
[6] M. Ishiguro, "Minimum redundancy linear arrays for a large number of antennas," *Radio Sci.*, vol. 15, pp. 1163–1170, Nov./Dec. 1980.
[7] S. Unnikrishna Pillai, Y. Bar-Ness, and F. Haber, "A new approach to array geometry for improved spatial spectrum estimation," *Proc. IEEE*, vol. 73, pp. 1522–1524, Oct. 1985.

[8] S. D. Bedrosian, "Nonuniform linear arrays: Graph-theoretic approach to minimum redundancy," *Proc. IEEE*, vol. 74, pp. 1040-1043, July 1986.
[9] S. W. Lang, G. L. Duckworth, and J. H. McClellan, "Array design for MEM and MLM array processing," in *Proc. IEEE ICASSP'81*, vol. 1, Mar. 1981, pp. 145-148.
[10] E. Vertatschitsch, S. Haykin, and K. M. Wong, "Optimum nonredundant arrays in beamforming," in *1983 Int. Electrical Electronics Conf.*, Tor., vol. 1, 1983, pp. 144-147.
[11] H. Taylor and S. W. Golomb, "Rulers Part 1," Univ. Southern California, Los Angeles, CSI Tech. Rep. 85-05-01, May 1985.
[12] E. Vertatschitsch and S. Haykin, "Nonredundant arrays," *Proc. IEEE*, vol. 74, p. 217, 1986.
[13] A. K. Dewdney, "Computer recreations: The search for an invisible ruler that will help radio astronomers to measure the earth," *Sci. Am.*, pp. 16-26, Dec. 1985.
[14] ——, "Computer recreations," *Sci. Am.*, pp. 14-21, Feb. 1986.
[15] H. L. Van Trees, *Detection, Estimation and Modulation Theory*, Part 1. New York: Wiley, 1968.
[16] E. J. Vertatschitsch, "Linear array structures for direction of arrival estimation," Ph.D. dissertation, McMaster Univ., Hamilton, ON, Canada, Nov. 1987.
[17] S. R. DeGraaf and D. H. Johnson, "Optimal linear arrays for narrowband beamforming," *ICASSP*, vol. 3, Mar. 1984, pp. 40.8.1-40.8.4.

Edward J. Vertatschitsch (S'82-M'85-S'86-M'86) was born in New York, NY, on May 19, 1958. He received the B.Sc. degree in physics and the Ph.D. degree in electrical engineering, all from McMaster University, Hamilton, Canada, in 1980 and 1987, respectively.

He has been with the High Technology Center of the Boeing Company, in Bellevue, WA, since 1987, where he has worked on the development of active, mm-wave, phased arrays and laser radars.

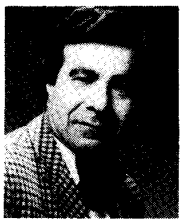

Simon Haykin (SM'70-F'82) received the B.Sc. (first class honours), Ph.D., and D.Sc. degrees, all in electrical engineering, from the University of Birmingham, England, in 1953, 1956, and 1967, respectively.

He is the founding Director of the Communications Research Laboratory and Professor of Electrical and Computer Engineering at McMaster University, Hamilton, ON, Canada. His research interests include neural networks, adaptive filters, and multidimensional signal processing with applications to radar.

Dr. Haykin was awarded the IEEE McNaughton Gold Medal (Region 7) in 1986.